A Satellite-Based Parameter to Monitor the Aerosol Impact on Convective Clouds

ITAMAR M. LENSKY

Department of Geography and Environment, Bar-Ilan University, Ramat-Gan, Israel

RON DRORI

Geography Department, The Hebrew University, Jerusalem, Israel

(Manuscript received 1 November 2005, in final form 8 June 2006)

ABSTRACT

A method to monitor the aerosol impact on convective clouds using satellite data is presented. The impacts of forest fires and highly polluting megacities on cloud precipitation formation processes are quantified by the vertical extent above cloud base to which convective cloud tops have to develop for onset of precipitation in terms of temperature difference D_{15}. Large D_{15} is a manifestation of the precipitation suppression effect of small cloud condensation nuclei aerosols that elevate the altitude where effective precipitation processes are initiated. A warmer land surface with a greater sensible heat flux that increases the updraft velocity at cloud base may also contribute to the same effect. Therefore, D_{15} is greater for clouds that develop over more polluted and/or warmer surfaces that result from smoke and urban pollution and/or urban heat island, respectively. The precipitation suppression effects of both smoke from forest fires and urban effects can be vividly seen in a case study over Southeast Asia. Typical values of D_{15} are 1°–6°C for tropical maritime clouds, 8°–15°C for tropical clouds over land, 16°–26°C for urban air pollution, and 18°–39°C for clouds ingesting smoke from forest fires.

1. Introduction

a. Aerosols and cloud formation processes

Aerosols alter warm, ice, and mixed-phase cloud formation processes by increasing droplet number concentrations and ice particle concentrations, decreasing the precipitation efficiency of warm clouds (Houghton et al. 2001). Aerosols that are dominated by submicron particles such as smoke, urban and industrial air pollution, and, sometimes, desert dust reduce the size of cloud droplets (Breon et al. 2002; Rosenfeld 1999, 2000) and suppress precipitation (Ramanathan et al. 2001). Freud et al. (2005) used in situ measurements in convective clouds over the Amazon basin to show that smoke from deforestation fires prevents clouds from precipitating until they acquire a vertical development of at least 4 km, as compared with only 1–2 km in clean clouds, and that the average cloud depth required for the onset of warm rain increased by ~350 m for each additional 100 cloud condensation nuclei per cubic centimeter at a supersaturation of 0.5%.

Khain et al. (2005) investigated physical mechanisms through which aerosols affect cloud microphysics, dynamics, and accumulated rain. They found that maritime aerosols bring about a rapid formation of raindrops that fall down through cloud updrafts, increasing the loading in the lower part of a cloud. They showed that an increase in the concentration of small cloud condensation nuclei leads to the formation of a large number of small droplets with a low collision rate, resulting in a time delay of raindrop formation. Such a delay prevents a decrease in the vertical velocity caused by the falling raindrops and thus increases the duration of the diffusion droplet growth stage, increasing latent heat release by condensation. The additional water that rises to the freezing level increases latent heat release by freezing. As a result, clouds developing in continental-type aerosol tend to have larger vertical velocities and tend to attain higher levels. Simulation of squall-

Corresponding author address: Dr. Itamar Lensky, The Department of Geography and Environmental Studies, Bar-Ilan University, Ramat-Gan 52900, Israel.
E-mail: lenskyi@mail.biu.ac.il

DOI: 10.1175/JAM2487.1

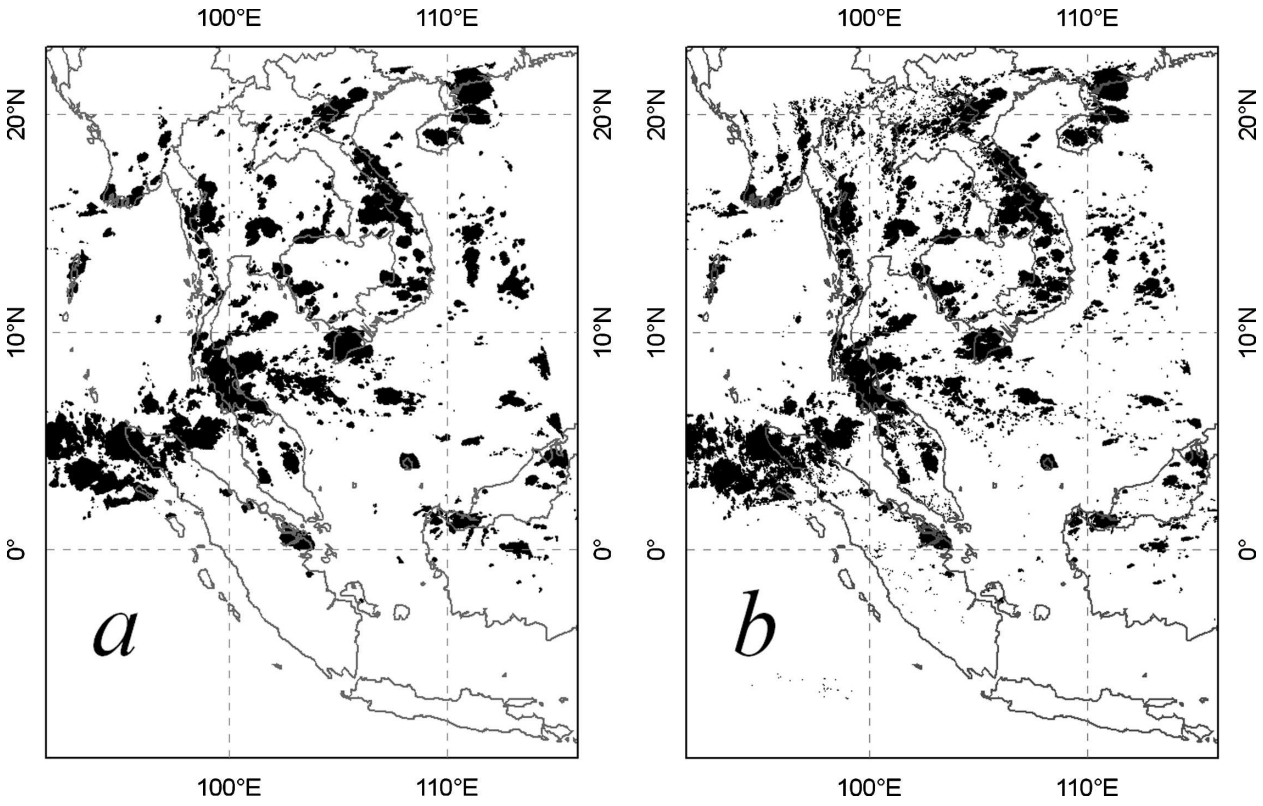

FIG. 1. Precipitation masks for (a) $T < 235$ K (GPI) and (b) $r_e \geq 15$ μm of NOAA AVHRR data from 14 Oct 1997 over Southeast Asia.

line formation showed that the clouds in the maritime aerosol cases did not produce strong downdrafts and did not lead to squall-line formation as do clouds developing under similar thermodynamic conditions with continental aerosol. The results of these simulations suggest that aerosols, which decrease the precipitation efficiency of most single clouds, can contribute to the formation of very intensive convective clouds and thunderstorms (squall lines, etc.) accompanied by very high precipitation rates.

It is therefore clear that there is a need for a technique to monitor the effect of cloud aerosol interactions on precipitation formation processes and that the connection of these processes to precipitation is complex. In this paper we suggest a simple parameter that gives indications on the precipitation formation processes using visible/infrared (VIS IR) satellite data.

b. Satellite-based rain estimates using VIS IR

Conventional ground-based rainfall data (rain gauges and weather radars) are limited in their extent of coverage and time span. This fact makes the attempt to measure precipitation from space so crucial (Levizzani et al. 2002). Among the VIS IR techniques, the simplest and perhaps most widely used technique is the one developed by Arkin (1979) during the Global Atmosphere Research Program Atlantic Tropical Experiment on the basis of a high correlation between radar-estimated precipitation and fraction of the area with cloud-top temperature T colder than 235 K in the IR wavelengths. The scheme, named the Geostationary Operational Environmental Satellite precipitation index (GPI; Arkin and Meisner 1987), assigns these areas a constant rain rate of 3 mm h^{-1}, which is appropriate for tropical precipitation over $2.5° \times 2.5°$ areas. It is obvious that the GPI misses warm rain.

One complementary approach to delineate rain and estimate rain intensity is based on the microphysical properties of cloud tops. Lensky and Rosenfeld (1997) and Albrecht (1989) used cloud-top particle effective radius r_e of 14–15 μm as a threshold for precipitation for both cold and warm processes. Rosenfeld et al. (2002) also found this threshold appropriate while using both observations (Visible and Infrared Scanner and precipitation radar on the Tropical Rainfall Measuring Mission satellite) and simulations of clean and polluted clouds. Figure 1 shows an example of rain delineation based on the GPI threshold of $T < 235$ K (Fig. 1a) and

on the threshold of $r_e \geq 15$ μm (Fig. 1b) of National Oceanic and Atmospheric Administration (NOAA) Advanced Very High Resolution Radiometer (AVHRR) Global Area Coverage data from 14 October 1997 over Southeast Asia. Note that in the microphysical rain delineation (Fig. 1b) warm clouds can be seen scattered along the figure while some of the cold clouds that were delineated as rain clouds in Fig. 1a are missing. The reason for the missing cold pixels is that two thresholds screening thin clouds (described in section 3) are checked before a pixel is assigned an effective radius.

These techniques are used to measure precipitation. However, they do not provide information on the precipitation formation processes that are crucial for the understanding of the effects of cloud–aerosol interactions on precipitation.

c. Retrieval of precipitation formation processes

Rosenfeld and Lensky (1998) suggested a technique to get insights into precipitation formation processes in continental and maritime convective clouds, based on analysis of the profiles of the effective radius with temperature (or height). They defined five microphysical zones that may be found in convective clouds. They demonstrated the ability to monitor transformation in the microphysical and precipitation-forming processes in convective clouds developing in air masses moving from the sea inland and in air masses moving into areas affected by biomass-burning smoke or urban air pollution.

The Rosenfeld–Lensky technique (RLT) is based on two assumptions. The first is that the r_e near cloud top for young clouds is similar to that well within the cloud at the same height of older clouds, as long as precipitation does not fall through that cloud volume. This assumption was verified using in situ aircraft measurements (Rosenfeld and Lensky 1998; Freud et al. 2005). The second assumption is that the evolution of r_e with height (or cloud-top temperature T), observed by the satellite at a given time (snapshot) for a cloud ensemble over an area, is similar to the T–r_e time evolution of a given cloud at one location. This is the ergodicity assumption, which implies exchangeability between the time and space domains. Lensky and Rosenfeld (2005) used Meteosat Second-Generation rapid-scan data (3-min interval) to examine the second assumption. The implication of the second assumption is that there must be enough clouds in different stages from young to mature in the selected area to allow a meaningful T–r_e plot to be constructed.

The RLT was widely accepted, and was followed by numerous papers by Rosenfeld and coauthors. However, it seems that it is still hard for other researchers to use this technique. This situation may be a result of three shortcomings of the RLT. First, it does not give a large-scale view but rather describes the precipitation formation processes in a cloud cluster in an area defined by the user. Second, the user must be skilled in selecting the area to be analyzed (such that a meaningful T–r_e plot may be constructed). Third, the user must know how to interpret the resulting T–r_e plot.

In this paper we propose a method that overcomes these three shortcomings. This method analyzes all of the available satellite data (full swath) rather than the limited area of the RLT, it is objective (it does not require a skilful user), and, as will be shown in the next section, the results are easy to interpret.

We suggest a parameter D_{15} that can provide a quantitative estimate of the impact of different surface properties and air masses (characterized by different aerosol types) on convective-cloud microstructure and precipitation formation processes. This parameter can be retrieved from standard operational visible/infrared satellite data.

In what follows, we proceed in three stages. The next section describes the parameter D_{15}. Then a case study is presented in section 3. Third, we discuss the possible contributions and limitations of using D_{15}.

2. The onset of precipitation in convective clouds

We define the temperature of the onset of precipitation in a window of 50×50 pixels as the temperature T_{15} at which the median r_e exceeds the precipitation threshold of 15 μm. Following the method of Lensky and Rosenfeld (1997), we define the cloud-base temperature T_{base} as the warmest cloudy pixel ($r_e > 0$) in the window. We define D_{15} as the difference between T_{15} and T_{base}:

$$D_{15} = T_{\text{base}} - T_{15}, \tag{1}$$

and we argue that D_{15} is a quantitative measure of the impact of different aerosols on precipitation formation processes.

The parameter D_{15} is a measure of how fast the rain develops in the convective elements. Under the same dynamical conditions, clouds with efficient rain formation processes will show small D_{15} while large D_{15} reveals that precipitation is suppressed. This difference is represented schematically in Fig. 2. In this figure three clouds are shown with the T–r_e diagram superimposed on them. A vertical dashed line indicates the 15-μm threshold for precipitation. The lower horizontal line represents T_{base}, and the upper line represents T_{15}. The gray rectangle represents the depth D_{15} (in terms of temperature difference) required for each cloud to de-

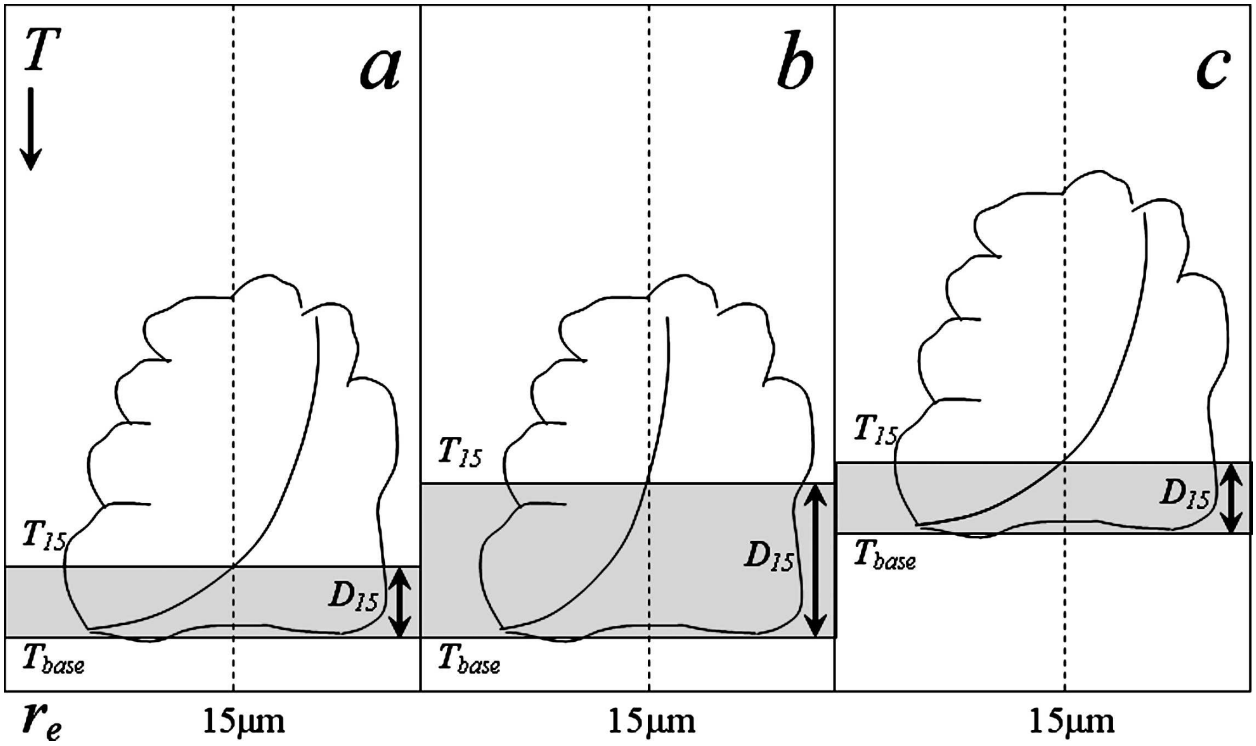

FIG. 2. Schematic representation of three clouds, with a T–r_e diagram superimposed on the clouds with a vertical dashed line that indicates the 15-μm threshold for precipitation. The lower horizontal line represents the cloud-base temperature, and the upper line represents the T_{15} temperature. The gray rectangle represents the depth D_{15} required for each cloud to develop precipitation formation processes. (a) A maritime cloud with warm cloud-base temperature and efficient precipitation formation processes, resulting in warm T_{15} temperature and small D_{15}. (b) A continental cloud with the same cloud-base temperature as the cloud in (a) but with a large diffusion growth zone, resulting in colder T_{15} temperature than the cloud in (a) and large D_{15}. (c) A cloud similar to the cloud in (a) but with cold cloud-base temperature and cold T_{15} temperature—nevertheless, the D_{15} is the same.

velop precipitation formation processes. Figure 2a shows a maritime cloud with warm cloud-base temperature and efficient precipitation formation processes, resulting in warm T_{15} temperature and small D_{15}. Figure 2b shows a continental cloud with the same cloud-base temperature as the cloud in Fig. 2a has but with a large diffusion growth zone, resulting in a colder T_{15} temperature than that for the cloud in Fig. 2a and large D_{15}. Figure 2c shows a cloud similar to the cloud in Fig. 2a but with cold cloud-base temperature and cold T_{15} temperature—nevertheless, the D_{15} is the same.

3. Case study

Full-resolution Local Area Coverage NOAA AVHRR data were used for the case study presented in this paper. Here D_{15} was calculated using r_e and the 10.8-μm channel brightness temperature. The 0.65-, 3.7-, 10.8-, and 12-μm channels were used to retrieve r_e (Rosenfeld and Lensky 1998). The cloudy pixels are pixels that passed the following thresholds (cloud mask): 0.6-μm reflectance greater than 50% (screening thin or broken clouds), 10.8-μm brightness temperature lower than ground temperature of 23°C, and maximum brightness temperature difference between 10.8 and 12 μm of 0.5°C (screening thin clouds).

To avoid unphysical results, several criteria were introduced. In a case in which the window is fully covered only with high cloud tops, the T_{15} will show very low temperature. To avoid such mistakenly low temperatures, a flag was given to a window in which the warmest cloudy pixel was colder than a predefined temperature threshold of −25°C, which is obviously not cloud base. Another criterion was added to avoid false interpretation in the case in which multilayer clouds are present in the window, such as thin cloud layers, partly covering the convective cloud layer. The nonconvective clouds were screened out using the fact that the r_e must increase with height in convective clouds and therefore r_e inversion indicates "contamination" by elevated layer clouds. This was done as in Lensky and Rosenfeld (1997).

A case study from 14 October 1997 illustrates the interaction of convective clouds with smoke over Sumatra and Kalimantan, Indonesia, and with air pollution from a few large cities. Figure 3 shows in the background a red–green–blue (RGB) composite of AVHRR channels 1 (0.6 μm) and 2 (0.8 μm) (red: channel 1, green: channel 2, and blue: channel 1). In this color scheme, the ocean appears black, vegetation appears green, the clouds appear white, and the smoke over Sumatra and Kalimantan is light purple. Parameter D_{15} is shown as an overlay of 111 $\times$ 80 windows of 50 $\times$ 50 pixels each. The red–orange colors represent maritime clouds with small D_{15} of 1°–6°C. These clouds can be seen over the South China Sea and the Andaman Sea. The green–yellow colors represent larger D_{15} of 10°–15°C over land (Thailand and Vietnam) resulting from the interaction of clouds with the continental surface and aerosols. Extremely large D_{15} (blue colors) can be seen over Bangkok, Thailand, (D_{15} = 26°C) and Ho Chi Minh City, Vietnam, (D_{15} = 22°C) and also over Phnom Penh, Cambodia, (D_{15} = 18°C) and Singapore (D_{15} = 17°C). Large D_{15} of 21°C can be seen also southwest of Ho Chi Minh City, resulting from northeasterly winds [from National Centers for Environmental Prediction (NCEP) reanalysis]. Two isolated large D_{15} can be seen over Ipoh (D_{15} = 17°C), the third largest city in Malaysia, and over Vinh (D_{15} = 27°C) in northern Vietnam; both cities have power plants. Dark blue colors representing much larger values of D_{15} of 18°–39°C, indicating highly suppressed precipitation-forming processes, can be found at the bottom of the figure, where clouds are influenced by the smoke aerosol. In the lower-left side of Fig. 3, shallow clouds with small D_{15} (2°–4°C) can be seen. The base of these clouds T_{base} is at 20°C, and cloud-top temperature is 16°–18°C. The NCEP reanalysis shows that 20°–17°C corresponds to 1.1–1.7 km above sea level. Hybrid Single-Particle Lagrangian Integrated Trajectory (HYSPLIT) 36-h back trajectories (Draxler and Rolph 2003) at levels of 500 (white dots), 1000 (gray dots), and 2000 (pink dots) m show that the smoke that is seen in the RGB composite of the AVHRR data is flowing over the cloud tops and that the clouds are being fed from clean maritime air, south of the smoke.

The patterns of D_{15} in Fig. 3 are different from those of the precipitation patterns in Fig. 1. It is obvious that Fig. 1 shows precipitation; however, we are interested in understanding the effect of aerosols on precipitation formation processes, which is precisely what D_{15} was constructed to monitor. It is notable that precipitation formation processes are revealed mainly by the younger clouds in the cloud cluster. Large anvils of mature clouds with cold tops and large r_e are used to estimate precipitation but do not contribute to retrieving the precipitation formation processes. These clouds can be seen in Fig. 1 but were rejected from the D_{15} analysis in Fig. 3 (clouds that do not have the D_{15} overlay). These figures yield two sets of information that are complementary.

4. Discussion and summary

This paper presents the method for and a case study of an objective algorithm for detection of the minimum depth above cloud base to which convective clouds have to develop for onset of precipitation, expressed in terms of a temperature difference called D_{15}. The analysis is performed on large-scale satellite data (full swath), with no need for a skilled user to define the area of the analysis. The results are quantitative, and they again do not require a skilled user to interpret them. Parameter D_{15} is most suitable for detecting the combined effects of dynamical and cloud aerosol interactions, because the effective radius is most sensitive to the depth above cloud base. Small D_{15} (1°–6°C) indicates that efficient warm-rain processes (i.e., coalescence and rainout) occur already in the lower parts of the clouds—typical of clouds that grow in clean air masses over the ocean or air from which aerosols were washed out by previous precipitation. Large D_{15} (8°–15°C) is typical of clouds growing in continental air masses, because of the combined effects of large concentrations of cloud condensation nuclei, lower relative humidity, and greater cloud-base updrafts relative to those over the ocean (Williams and Stanfill 2002). These delineations are demonstrated in Fig. 3, where rapid shift of clouds from "maritime" to "continental" can be seen. Extremely large D_{15} are typical of clouds growing in polluted air: 16°–26°C for an urban area that combines the effects of heat island and air pollution and 18°–39°C for clouds ingesting smoke from forest fires. This result suggests that the impact of urban air pollution on clouds is almost as great as that of smoke from forest fires. It should be borne in mind that D_{15} is not linear throughout the whole range of clouds. Indeed, time delay of raindrop formation may indicate suppressed precipitation. However, aerosol-laden clouds that did grow above the freezing level were observed to be more vigorous (Rosenfeld and Woodley 2003) and to have larger ice hydrometeor mass at the expense of suppressed warm rain, leading to extreme hail reaching the surface (Andreae et al. 2004). Therefore, although D_{15} reveals much information regarding cloud–aerosol interactions and their impact on precipitation formation processes, more research is needed to be done before this result can be translated to an improved quantitative VIS IR precipitation algorithm.

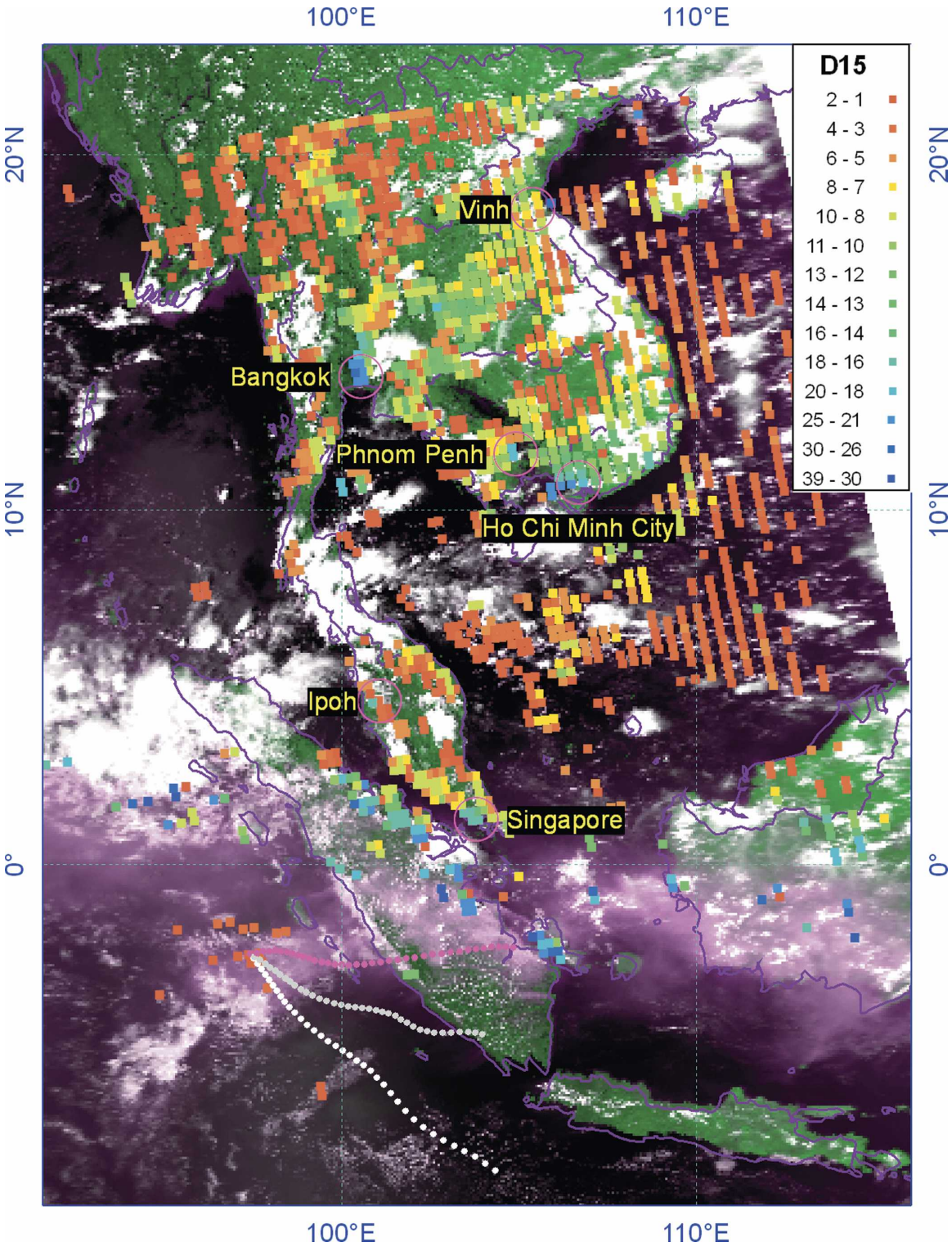

FIG. 3. In the background is an RGB composition of NOAA AVHRR channels 1 (0.6 μm; red and blue) and 2 (0.8 μm; green) from 14 Oct 1997 over Southeast Asia. In this RGB combination, the ocean is black, vegetation is green, clouds are white, and the smoke (near the equator) is purple. An overlay of D_{15} shows clouds from clean maritime air with low D_{15} (red), clouds with larger D_{15} (green–yellow) over land, and extremely large D_{15} (blue colors) that can be seen over Bangkok, Ho Chi Minh City, Phnom Penh, Singapore, Ipoh, and Vinh; much larger D_{15} (dark blue) is indicating highly suppressed precipitation-forming processes, where clouds are influenced by the smoke aerosol. The trajectories are described in the text.

Acknowledgments. The authors are grateful for constructive suggestions from the reviewers. This research has been obtained from the cooperation between the Hebrew University of Jerusalem and NASDA in ADEOS-II Research activity and was supported by the Schnitzer Foundation for Research on the Israeli Economy and Society. The authors gratefully acknowledge the NOAA Air Resources Laboratory for the provision of the HYSPLIT transport and dispersion model Web site (http://www.arl.noaa.gov/ready.html) used in this publication. NCEP reanalysis data were provided by the NOAA–CIRES Climate Diagnostics Center in Boulder, Colorado, from their Web site (http://www.cdc.noaa.gov/). The data source for the case study is from The Comprehensive Large Array-Data Stewardship System (CLASS; information online at http://www.class.noaa.gov/).

REFERENCES

Albrecht, B. A., 1989: Aerosols, cloud microphysics and fractional cloudiness. *Science,* **245,** 1227–1230.

Andreae, M. O., D. Rosenfeld, P. Artaxo, A. A. Costa, G. P. Frank, K. M. Longo, and M. A. F. Silva-Dias, 2004: Smoking rain clouds over the Amazon. *Science,* **303,** 1337–1342.

Arkin, P. A., 1979: The relationship between fractional coverage of high cloud and rainfall accumulations during GATE over the B-scale array. *Mon. Wea. Rev.,* **107,** 1382–1387.

——, and B. N. Meisner, 1987: The relationship between large-scale convective rainfall and cold cloud over the Western Hemisphere during 1982–84. *Mon. Wea. Rev.,* **115,** 51–74.

Breon, F.-M., D. Tanre, and S. Generoso, 2002: Aerosol effect on cloud droplet size monitored from satellite. *Science,* **295,** 834–838.

Draxler, R. R., and G. D. Rolph, cited 2003: NOAA ARL HYSPLIT model overview. NOAA Air Resources Laboratory. [Available online at http://www.arl.noaa.gov/ready/hysplit4.html.]

Freud, E., D. Rosenfeld, M. O. Andreae, A. A. Costa, and P. Artaxo, 2005: Robust relations between CCN and the vertical evolution of cloud drop size distribution in deep convective clouds. *Atmos. Chem. Phys. Discuss.,* **5,** 10 155–10 195.

Houghton, J. T., Y. Ding, D. J. Griggs, M. Noguer, P. J. van der Linden, X. Dai, K. Maskell, and C. A. Johnson, Eds., 2001: *Climate Change 2001: The Scientific Basis.* Cambridge University Press, 881 pp.

Khain, A., D. Rosenfeld, and A. Pokrovsky, 2005: Aerosol impact on the dynamics and microphysics of convective clouds. *Quart. J. Roy. Meteor. Soc.,* **131,** 2639–2663.

Lensky, I. M., and D. Rosenfeld, 1997: Estimation of precipitation area and rain intensity based on the microphysical properties retrieved from NOAA AVHRR data. *J. Appl. Meteor.,* **36,** 234–242.

——, and ——, 2005: The time–space exchangeability of satellite retrieved relations between cloud top temperature and particle effective radius. *Atmos. Chem. Phys. Discuss.,* **5,** 11 911–11 928.

Levizzani, V., R. Amorati, and F. Meneguzzo, 2002: A review of satellite-based rainfall estimation methods. European Commission Project MUSIC Rep. EVK1-CT-2000-00058, 66 pp.

Ramanathan, V., P. J. Crutzen, J. T. Kiehl, and D. Rosenfeld, 2001: Aerosols, climate and the hydrological cycle. *Science,* **294,** 2119–2124.

Rosenfeld, D., 1999: TRMM observed first direct evidence of smoke from forest fires inhibiting rainfall. *Geophys. Res. Lett.,* **26,** 3105–3108.

——, 2000: Suppression of rain and snow by urban and industrial air pollution. *Science,* **287,** 1793–1796.

——, and I. M. Lensky, 1998: Satellite-based insights into precipitation formation processes in continental and maritime convective clouds. *Bull. Amer. Meteor. Soc.,* **79,** 2457–2476.

——, and W. L. Woodley, 2003: Closing the 50-year circle: From cloud seeding to space and back to climate change through precipitation physics. *Cloud Systems, Hurricanes, and the Tropical Rainfall Measuring Mission (TRMM), Meteor. Monogr.,* No. 51, Amer. Meteor. Soc., 59–80.

——, R. Lahav, A. P. Khain, and M. Pinsky, 2002: The role of sea-spray in cleansing air pollution over ocean via cloud processes. *Science,* **297,** 1667–1670.

Williams, E. R., and S. Stanfill, 2002: The physical origin of the land–ocean contrast in lightning activity. *Appl. Phys.,* **3,** 1277–1292.